AD-A197 716

REPORT DOCUMENTATION PAGE

DTIC ELECTE AUG 19 1988 H

Unclassified	1b. RESTRICTIVE MARKINGS
2a. SECURITY CLASSIFICATION AUTHORITY	3. DISTRIBUTION / AVAILABILITY OF REPORT
2b. DECLASSIFICATION / DOWNGRADING SCHEDULE	
4. PERFORMING ORGANIZATION REPORT NUMBER(S) AFGL-TR-88-0171	5. MONITOPING ORGANIZATION REPORT NUMBER(S)
6a. NAME OF PERFORMING ORGANIZATION Air Force Geophysics Laboratory	6b. OFFICE SYMBOL (*If applicable*) PHS
6c. ADDRESS (*City, State, and ZIP Code*) Hanscom AFB Massachusetts, 01731-5000	7a. NAME OF MONITORING ORGANIZATION
8a. NAME OF FUNDING / SPONSORING ORGANIZATION	8b. OFFICE SYMBOL (*If applicable*)
8c. ADDRESS (*City, State, and ZIP Code*)	7b. ADDRESS (*City, State, and ZIP Code*)
	9. PROCUREMENT INSTRUMENT IDENTIFICATION NUMBER

10. SOURCE OF FUNDING NUMBERS

PROGRAM ELEMENT NO	PROJECT NO.	TASK NO.	WORK UNIT ACCESSION NO.
61102F	2311	G3	22

11. TITLE (*Include Security Classification*)
Signal Transfer Function of the Knox-Thompson Speckle Imaging Technique

12. PERSONAL AUTHOR(S)
Oskar von der Luhe

13a. TYPE OF REPORT	13b. TIME COVERED	14. DATE OF REPORT (*Year, Month, Day*)	15. PAGE COUNT
Reprint	FROM _____ TO _____	1988 August 15	9

16. SUPPLEMENTARY NOTATION
Reprinted from Journal of the Optical Society of America A, Vol. 5, page 721, May 1988

17. COSATI CODES		
FIELD	GROUP	SUB-GROUP

18. SUBJECT TERMS (*Continue on reverse if necessary and identify by block number*)
Speckle interferometry, Reprints,

19. ABSTRACT (*Continue on reverse if necessary and identify by block number*)

The transfer function associated with the Knox-Thompson speckle imaging technique is investigated. Numerical model transfer functions using log-normal statistics for perturbations of the complex wave front, the near-field approximation, and a Kolmogorov spectrum for atmospheric turbulence statistics are presented. Simple approximations for the transfer function are discussed. As with the transfer function of Labeyrie's speckle interferometry technique, the portion beyond the seeing limit can be represented as the transfer function of an unaberrated telescope times a seeing-dependent constant. An additional factor depends on the frequency shift of the Knox-Thompson cross spectra. The influence of the frequency shift on the reconstructed phase error is discussed for simple reconstruction problems.

Reprints

DISTRIBUTION STATEMENT A
Approved for public release;
Distribution Unlimited

20. DISTRIBUTION / AVAILABILITY OF ABSTRACT	21. ABSTRACT SECURITY CLASSIFICATION
☐ UNCLASSIFIED/UNLIMITED ☒ SAME AS RPT. ☐ DTIC USERS	Unclassified

22a. NAME OF RESPONSIBLE INDIVIDUAL	22b. TELEPHONE (*Include Area Code*)	22c. OFFICE SYMBOL
Claire Caulfield	(617) 377-4555	SULLP

DD FORM 1473, 84 MAR — 83 APR edition may be used until exhausted. All other editions are obsolete.

SECURITY CLASSIFICATION OF THIS PAGE
Unclassified

Reprinted from Journal of the Optical Society of America A, Vol. 5, page 721, May 1988

Signal transfer function of the Knox–Thompson speckle imaging technique

Oskar von der Lühe

Solar Research Branch, U.S. Air Force Geophysics Laboratory, Sacramento Peak, Sunspot, New Mexico 88349

Received May 6, 1987; accepted January 13, 1988

The transfer function associated with the Knox–Thompson speckle imaging technique is investigated. Numerical model transfer functions using log-normal statistics for perturbations of the complex wave front, the near-field approximation, and a Kolmogorov spectrum for atmospheric turbulence statistics are presented. Simple approximations for the transfer function are discussed. As with the transfer function of Labeyrie's speckle interferometry technique, the portion beyond the seeing limit can be represented as the transfer function of an unaberrated telescope times a seeing-dependent constant. An additional factor depends on the frequency shift of the Knox–Thompson cross spectra. The influence of the frequency shift on the reconstructed phase error is discussed for simple reconstruction problems.

1. INTRODUCTION

The Knox–Thompson[1] (KT) speckle imaging technique plays a significant role in present methods of high-resolution optical astronomical imaging. Speckle imaging techniques permit the recovery of small-scale information on astronomical sources that normally is destroyed by the deleterious effect of turbulence in the Earth's atmosphere on the imaging process. Unlike Labeyrie's[2] speckle interferometry, which measures the autocorrelation of the observed intensity distribution, the KT technique permits the recovery of the full information on the observed intensity structure. Because the technique is relatively simple to apply compared with other techniques, such as speckle masking,[3] it has found wide application in high-resolution imaging astronomy, ranging from stellar sources[4] to extended objects, such as the Sun.[5]

In speckle interferometry and speckle imaging, a large number of short-exposure pictures of the source of interest are taken. Each picture is affected by atmospheric turbulence, and if the exposure is short compared with the atmospheric correlation time (of the order of 10 msec), the observed intensity distribution of the ith picture, I_i, may be represented by the true, unaberrated intensity distribution, I_0, convolved by a randomly speckled point-spread function, PSF_i, which typically spreads over 1 arcsec:

$$I_i(\mathbf{x}) = I_0(\mathbf{x}) * \mathrm{PSF}_i(\mathbf{x}), \tag{1}$$

where $\mathbf{x}$ denotes a two-dimensional focal-plane coordinate and $*$ denotes the convolution operation. When long exposures are taken, the speckles average out, and the effective point-spread function is smooth and does not permit the recovery of detail smaller than its average diameter x_s, called the seeing limit.

The speckles in the point-spread function are of the size of the theoretical resolution element of the instrument, and a suitable statistical analysis of their modulation permits the recovery of object structure information up to the resolution limit. Such an analysis is frequently done in the Fourier domain. If F_i and F_0 are the two-dimensional Fourier transforms of I_i and I_0, respectively, then

$$F_i(\mathbf{f}) = F_0(\mathbf{f})S_i(\mathbf{f}), \tag{2}$$

for which S_i denotes the instantaneous optical transfer function, i.e., the Fourier transform of $\mathrm{PSF}_i(\mathbf{x})$, which depends on the telescope and the atmosphere, and $\mathbf{f}$ denotes a two-dimensional spatial frequency. The essence of the KT technique is to evaluate the average

$$\frac{1}{N}\sum_{i=1}^{N} F_i(\mathbf{f})F_i^*(\mathbf{f}-\Delta) = F_0(\mathbf{f})F_0^*(\mathbf{f}-\Delta) \times \frac{1}{N}\sum_{i=1}^{N} S_i(\mathbf{f})S_i^*(\mathbf{f}-\Delta) \tag{3}$$

for a fixed spatial-frequency spacing Δ. N is the number of Fourier transforms processed. Both sides of Eq. (3) are complex functions. There is some controversy about what to call quantities such as $F(\mathbf{f})F^*(\mathbf{f}-\Delta)$; the term cross spectrum seems to prevail, so I shall use it throughout this paper.

Equation (3) shows that the observed average cross spectrum is given by the object cross spectrum multiplied by an average telescopic–atmospheric term, the cross-spectrum transfer function (CTF). Knox and Thompson[1] realized that, in the ensemble-average limit $N \to \infty$, the CTF is a purely real function as long as Δ is small compared with the seeing cutoff frequency f_s, which is reciprocal to the seeing limit x_s. The Fourier phase of the observed cross spectrum is equal to the phase of the object cross spectrum; the object Fourier phase may be recovered from the observed cross-spectrum phase by means of suitable integration techniques. If the CTF is known, Fourier amplitudes may be also recovered from the cross spectra [Eq. (3)]; amplitudes and phases can be recombined and inversely transformed to obtain the reconstructed object intensity distribution. Because of the better signal-to-noise ratio, Fourier amplitudes are commonly obtained by using Labeyrie's[2] method of analyzing

0740-3222/88/050721-09$02.00

cross spectra for $\Delta = 0$ (referred to as the Labeyrie case in this paper).

The accuracy to which phases can be recovered from observed cross spectra depends on Δ, because the amplitudes of the observed cross spectra decrease as Δ increases. As a rule of thumb, Knox and Thompson[1] require that Δ be smaller than $0.5\,f_s$; Fried[6] requires that $\Delta < 0.2\,f_s$. A more accurate description of how cross spectra amplitudes are affected by the choice of Δ is required in order to study the dependence of phase errors on Δ. Also, the choice of Δ imposes a lower limit on the size of the observed field of view. If an extended source, such as the solar surface, is observed, a small field of view is required in order to match the size of the isoplanatic patch.[6,7] Once the field size is selected, Δ cannot be made smaller than the fundamental frequency given by that size, and it is conceivable that under unfavorable seeing conditions the KT algorithm will fail. Also, variations of the KT technique use sets of cross spectra with varying Δ,[8] and in these cases it is important to know how large the modulus of Δ can be made without penalty.

In this paper I present an extension of Korff's[9] approach for deriving the transfer function associated with the Labeyrie technique to the transfer function that determines the signal of the KT technique. Neither Korff's result nor the general solution has an analytical expression, and each must be calculated numerically. Results of such calculations are presented for a circular, unocculted entrance pupil of an aberration-free telescope. In addition, approximations for the cases of small and large spatial frequencies are discussed, which permit a simpler estimate of the loss of cross-spectrum signal as Δ is increased.

The treatment described here is based on the assumption of log-normal statistics for the complex wave amplitude perturbations, the near-field approximation,[9-11] and a Kolmogorov spectrum for atmospheric turbulence.[12] Barakat *et al.*[13] discussed the influence of aberrations of atmospheric as well as instrumental origin on KT cross-spectrum phases for a one-dimensional entrance pupil. They assumed a Gaussian correlation function to describe the second-order statistics of wave-front perturbations. Such an analysis is certainly adequate for the study of the effects of instrumental aberration. I largely neglect those in this paper, and I concentrate on the effects of atmospheric turbulence for a two-dimensional entrance pupil. The assumptions for the wave-front statistics that I use are generally believed to be more relevant to astronomical observations,[11] and there is substantial observational evidence to support them.[14,15] An excellent treatment of the statistics of wave-front perturbations caused by turbulent media can be found in the review by Bertolotti *et al.*[16]

2. NOTATION

By using log-normal statistics and near-field conditions,[9,10] the instantaneous optical transfer function in a symmetrical formulation may be expressed as

$$S_i(\mathbf{f}) = \int\int W\left(\mathbf{r} + \frac{\lambda\mathbf{f}}{2}\right) W^*\left(\mathbf{r} - \frac{\lambda\mathbf{f}}{2}\right) \times \exp\left\{j\left[\phi_i\left(\mathbf{r} + \frac{\lambda\mathbf{f}}{2}\right) - \phi_i\left(\mathbf{r} - \frac{\lambda\mathbf{f}}{2}\right)\right]\right\} d\mathbf{r}. \quad (4)$$

$W(\mathbf{r})$ denotes the complex amplitude transmittance of the telescope's entrance pupil and describes the telescope aberrations. $\phi_i(\mathbf{r})$ denotes the instantaneous phase retardation that is due to atmospheric turbulence. $\mathbf{r}$ denotes a two-dimensional pupil-plane coordinate. The coordinate $\mathbf{f}$ represents a two-dimensional angular frequency with units of line pairs per radian. λ is the light wavelength and $j = \sqrt{-1}$. The statistics of the random wave-front perturbations are represented by the phase structure function $\mathbf{D}(\rho)$, defined as

$$\mathbf{D}(\rho) = \langle[\phi(\mathbf{r}) - \phi(\mathbf{r} - \rho)]^2\rangle. \quad (5)$$

Angle brackets denote ensemble averaging. We shall use Fried's[10] expression for the structure function, which is based on a Kolmogorov spectrum of atmospheric turbulence[12]:

$$\mathbf{D}(\rho) = 6.88\left(\frac{|\rho|}{r_0}\right)^{5/3}. \quad (6)$$

r_0 is Fried's seeing parameter and is related to the angular seeing cutoff frequency by $f_s = r_0/\lambda$. Occasionally, we shall use the fact that Eq. (6) depends only on the modulus $|\rho|$.

In order to simplify the mathematical expressions without suffering a loss of generality, we shall redefine coordinates. We measure angular frequencies in units of the cutoff frequency of the instrument, $f_c = D/\lambda$, where D is the entrance pupil diameter, and we then set $D = 1$. The new Fourier-space variable is now $\mathbf{q} = \lambda\mathbf{f}/D = \lambda\mathbf{f}$, and, for the frequency region of interest, $0 \leq |\mathbf{q}| \leq 1$, where $|\mathbf{q}|$ represents the magnitude of the two-dimensional vector $\mathbf{q}$. Also, Fried's parameter is measured in units of the telescope diameter, so we set $\alpha = r_0/D$. We can express Eq. (4) in these variables and obtain

$$S_i(\mathbf{q}) = \int\int W(\mathbf{r} + \mathbf{q}/2) W^*(\mathbf{r} - \mathbf{q}/2) \times \exp\{j[\phi_i(\mathbf{r} + \mathbf{q}/2) - \phi_i(\mathbf{r} - \mathbf{q}/2)]\} d\mathbf{r}. \quad (7)$$

The domain of integration is limited by the terms W, which vanish outside the area of the entrance pupil, i.e., for $|\mathbf{r}| > 1/2$. The structure function, recast in the new variables, becomes

$$\mathbf{D}(\rho) = 6.88\left(\frac{|\rho|}{\alpha}\right)^{5/3}. \quad (8)$$

3. DERIVATION OF THE SIGNAL TRANSFER FUNCTION

The objective of this section is to derive the ensemble average of the transfer function $\mathrm{CTF}_\Delta(\mathbf{q})$ of the cross-spectrum signal by using Eq. (7). The general result is presented in Subsection 3.A, Eq. (11). Approximations of the cases for small and large spatial frequencies are discussed in Subsection 3.B; the results are presented in Eqs. (20) and (27), respectively. A description of the numerical evaluation of Eq. (11) is given in Subsection 3.C.

A. General Analysis

From Eq. (3), it is seen that the CTF is given by

$$\mathrm{CTF}_\Delta(\mathbf{q}) = \langle S_i(\mathbf{q}) S_i^*(\mathbf{q} - \Delta)\rangle. \quad (9)$$

For convenience, we drop the frame number index i in ensemble-average expressions. Inserting Eq. (7) into Eq. (9) yields

$$\mathrm{CTF}_\Delta(\mathbf{q}) = \Big\langle \int\int W(\mathbf{r}+\mathbf{q}/2)W^*(\mathbf{r}-\mathbf{q}/2) \times \exp\{j[\phi(\mathbf{r}+\mathbf{q}/2)-\phi(\mathbf{r}-\mathbf{q}/2)]\}\mathrm{d}\mathbf{r} \times \int\int W^*[\mathbf{r}'+(\mathbf{q}-\Delta)/2]W[\mathbf{r}'-(\mathbf{q}-\Delta)/2] \times \exp\{j[-\phi[\mathbf{r}'+(\mathbf{q}-\Delta)/2] + \phi[\mathbf{r}'+(\mathbf{q}-\Delta)/2]\}\mathrm{d}\mathbf{r}' \Big\rangle. \quad (10)$$

The general result for the transfer function of KT cross spectra is obtained in Appendix A by extending Korff's[9] derivation to nonzero-frequency offsets Δ. The final result is given by

$$\mathrm{CTF}_\Delta(\mathbf{q}) = \int\int\int\int W\left(\frac{\sigma+\delta+\mathbf{q}}{2}\right)W^*\left(\frac{\sigma+\delta-\mathbf{q}}{2}\right) \times W^*\left(\frac{\sigma-\delta+\mathbf{q}-\Delta}{2}\right)W\left(\frac{\sigma-\delta-\mathbf{q}+\Delta}{2}\right)\mathrm{d}\sigma \times \exp\{-\tfrac{1}{2}[\mathbf{D}(\mathbf{q})+\mathbf{D}(\mathbf{q}-\Delta)+\mathbf{D}(\delta+\Delta/2) + \mathbf{D}(\delta-\Delta/2)-\mathbf{D}(\mathbf{q}-\Delta/2+\delta) - \mathbf{D}(\mathbf{q}-\Delta/2-\delta)]\}\mathrm{d}\delta. \quad (11)$$

Korff's result is reproduced in Eq. (11) if Δ is set to zero. The first part, the integral over σ, contains purely instrumental terms; it may be represented as the overlap area of four circles (or annuli) representing the transparent portions of the entrance pupil if there are no aberrations. In contrast to Korff's result, however, the centers of the four pupils are not located on the corners of a parallelogram; two of the pupils are shifted by the cross-spectrum term $\Delta/2$ (see Fig. 1). Equation (11) has no analytic solution if Eq. (8) is used for the structure function, and therefore Eq. (11) must be solved numerically.

B. Approximations and Special Cases

1. The Signal at $\mathbf{q} = 0$

Setting $\mathbf{q} = 0$ in Eq. (11) yields

$$\mathrm{CTF}_\Delta(0) = \int\int\int\int \left|W\left(\frac{\sigma+\delta}{2}\right)\right|^2 W^*\left(\frac{\sigma-\delta-\Delta}{2}\right) \times W\left(\frac{\sigma-\delta+\Delta}{2}\right)\mathrm{d}\sigma\mathrm{d}\delta \exp[-\tfrac{1}{2}\mathbf{D}(\Delta)]. \quad (12)$$

If we restore variables $\mathbf{r}$ and $\mathbf{r}'$ [see Eq. (A7) in Appendix A], we obtain

$$\mathrm{CTF}_\Delta(0) = \int\int |W(\mathbf{r})|^2\mathrm{d}\mathbf{r} \int\int W^*(\mathbf{r}'-\Delta/2) \times W(\mathbf{r}'+\Delta/2)\mathrm{d}\mathbf{r}' \exp[-\tfrac{1}{2}\mathbf{D}(\Delta)]. \quad (13)$$

The first integral represents merely the area of the entrance pupil if its transparency is unity. The second integral might be found to be a complex number and thus might represent a systematic error term if the telescope has aberrations and therefore W is complex. If aberrations are disregarded, the second integral represents the overlap area of two pupils separated by Δ. The exponential represents the atmospheric contribution to the signal at zero frequency.

To illustrate this result, let us assume an aberration-free telescope with a circular, unobscured entrance pupil, for which

$$W(\mathbf{r}) = \Pi(\mathbf{r}) \equiv \begin{cases} 1 & \text{if } |\mathbf{r}| < \tfrac{1}{2} \\ \tfrac{1}{2} & \text{if } |\mathbf{r}| = \tfrac{1}{2} \\ 0 & \text{if } |\mathbf{r}| > \tfrac{1}{2} \end{cases}. \quad (14)$$

The signal at zero frequency then becomes

$$\mathrm{CTF}_\Delta(0) = \frac{\pi}{8}[\cos^{-1}\Delta - \Delta(1-\Delta^2)^{1/2}]\exp\left[-3.44\left(\frac{\Delta}{\alpha}\right)^{5/3}\right]. \quad (15)$$

Equations (14) and (15) indicate that, compared with the Labeyrie case for which $\Delta = 0$, the signal decreases with increasing Δ. In what follows, the area-normalized signal transfer function will be presented, which is unity at the frequency origin for the Labeyrie case. This presentation permits us to assess correctly the loss of signal over the entire frequency range as Δ is increased.

2. The Signal at Small Spatial Frequencies

The regime for small spatial frequencies $|\mathbf{q}| \ll \alpha$ can be approximated by expanding the sum of structure functions in Eq. (11) into a power series. The basic expansion of the structure function [Eq. (6)], up to second order, is given by

$$6.88\left(\frac{\mathbf{x}+\epsilon}{\alpha}\right)^{5/3} \approx 6.88\left(\frac{\mathbf{x}}{\alpha}\right)^{5/3}\left\{1+\frac{5}{6}\left[\frac{|\epsilon|}{|\mathbf{x}|}\cos\theta + \left(\frac{|\epsilon|}{|\mathbf{x}|}\right)^2\left(1-\frac{1}{12}\cos^2\theta\right)+\cdots\right]\right\}, \quad (16)$$

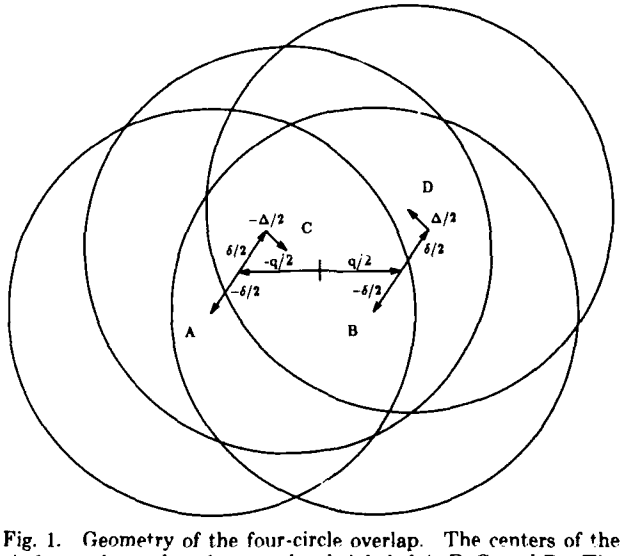

Fig. 1. Geometry of the four-circle overlap. The centers of the circles are located at the arrowheads labeled A, B, C, and D. The arrows indicate the magnitude and direction of the vectors $\mathbf{q}$, δ, and Δ. In the case shown here, the overlap area is determined by only the three circles A, B, and D.

where θ is the angle beween the vectors $\mathbf{x}$ and ϵ and $|\mathbf{x}| \gg |\epsilon|$. Using relation (16), the sum of structure terms Σ in the exponent in Eq. (11) may be expressed, up to first order in $\mathbf{q}$ about $\delta \pm \Delta/2$, as

$$\sum \approx 6.88\left\{\left(\frac{\mathbf{q}}{\alpha}\right)^{5/3} + \left(\frac{|\mathbf{q}-\Delta|}{\alpha}\right)^{5/3} + \frac{5}{6}\left[\frac{|\mathbf{q}|}{|\delta-\Delta/2|}\cos\theta'\left(\frac{|\delta-\Delta/2|}{\alpha}\right)^{5/3} - \frac{|\mathbf{q}|}{|\delta+\Delta/2|}\cos\theta\left(\frac{|\delta+\Delta/2|}{\alpha}\right)^{5/3}\right]\right\}. \quad (17)$$

θ is the angle between $\mathbf{q}$ and $\delta + \Delta/2$, and θ' is the angle between $\mathbf{q}$ and $\delta - \Delta/2$. In general, $|\Delta|$ will be of order α. If we assume that $\alpha \ll 1$, we may approximate $\delta - \Delta \approx \delta$ and $\theta' \approx \theta$ for most part of the δ integration. Hence, up to first order,

$$\sum \approx 6.88\left[\left(\frac{\mathbf{q}}{\alpha}\right)^{5/3} + \left(\frac{|\mathbf{q}-\Delta|}{\alpha}\right)^{5/3}\right]. \quad (18)$$

Therefore the turbulence contribution falls out of the integration, and

$$\mathrm{CTF}_\Delta(\mathbf{q}) \approx \int\int\int\int W\left(\frac{\sigma+\delta+\mathbf{q}}{2}\right) W^*\left(\frac{\sigma+\delta-\mathbf{q}}{2}\right) \times W^*\left(\frac{\sigma-\delta+\mathbf{q}-\Delta}{2}\right) W\left(\frac{\sigma-\delta-\mathbf{q}+\Delta}{2}\right) \mathrm{d}\sigma\mathrm{d}\delta \times \exp\left\{-3.44\left[\left(\frac{\mathbf{q}}{\alpha}\right)^{5/3} + \left(\frac{|\mathbf{q}-\Delta|}{\alpha}\right)^{5/3}\right]\right\}. \quad (19)$$

The evaluation of the integrals results in the product of the aberration-limited telescopic transfer function $S_{t,a}$ at spatial frequencies $\mathbf{q}$ and $\mathbf{q} - \Delta$. If we disregard instrumental aberrations and use Fried's[9] result for the average long-exposure transfer function $S_{\mathrm{LE}}(\mathbf{q})$, we finally obtain

$$\mathrm{CTF}_\Delta(\mathbf{q})|_{|\mathbf{q}|\ll\alpha} \approx S_{t,a}(\mathbf{q})\exp\left[-3.44\left(\frac{|\mathbf{q}|}{\alpha}\right)^{5/3}\right] S_{t,a}{}^*(\mathbf{q}-\Delta) \times \exp\left[-3.44\left(\frac{|\mathbf{q}-\Delta|}{\alpha}\right)^{5/3}\right] \approx S_{\mathrm{LE}}(\mathbf{q}) S_{\mathrm{LE}}(\mathbf{q}-\Delta). \quad (20)$$

3. *The Signal at Large Spatial Frequencies*

We now assume that $|\mathbf{q}| \gg \alpha$, and, by using expansion (16), we find, for the sum Σ of exponentials in Eq. (11) up to second order in δ,

$$\sum \approx 6.88\left[\left(\frac{|\delta+\Delta/2|}{\alpha}\right)^{5/3} + \left(\frac{|\delta-\Delta/2|}{\alpha}\right)^{5/3} + \left(\frac{\mathbf{q}}{\alpha}\right)^{5/3} + \left(\frac{\mathbf{q}-\Delta}{\alpha}\right)^{5/3} - 2\left(\frac{\mathbf{q}-\Delta/2}{\alpha}\right)^{5/3} + \frac{5}{3}\frac{\delta^2}{|\mathbf{q}-\Delta/2|^2}\left(1-\frac{1}{12}\cos^2\theta\right)\right]. \quad (21)$$

Here θ is the angle between $\mathbf{q} - \Delta/2$ and δ. Again, Δ will be of order α and small compared with $\mathbf{q}$. Therefore it is justified to assume that $\mathbf{q} - \Delta \approx \mathbf{q} - \Delta/2 \approx \mathbf{q}$. In this case, the terms involving $\mathbf{q}$ cancel, and an approximation to Σ, to first order in δ, is given by

$$\sum \approx 6.88\left[\left(\frac{|\delta+\Delta/2|}{\alpha}\right)^{5/3} + \left(\frac{|\delta-\Delta/2|}{\alpha}\right)^{5/3}\right]. \quad (22)$$

In order to proceed further, we assume that instrumental aberrations are small compared with atmospheric wavefront distortions or, equivalently, that $W(\mathbf{r})$ is essentially constant over areas with a typical size α. Since the exponential contributes to the integration only if $\delta \leq \alpha$, the δ variable may be neglected in arguments of W for most parts of the σ integration. We may then separate δ integration from σ integration, and we obtain

$$\mathrm{CTF}_\Delta(\mathbf{q}) \approx \int\int W\left(\frac{\sigma+\mathbf{q}}{2}\right) W^*\left(\frac{\sigma-\mathbf{q}}{2}\right) \times W^*\left(\frac{\sigma+\mathbf{q}-\Delta}{2}\right) W\left(\frac{\sigma-\mathbf{q}+\Delta}{2}\right) \mathrm{d}\sigma \times \int\int \exp\left\{-3.44\left[\left(\frac{|\delta+\Delta/2|}{\alpha}\right)^{5/3} + \left(\frac{|\delta-\Delta/2|}{\alpha}\right)^{5/3}\right]\right\} \mathrm{d}\delta. \quad (23)$$

We first consider the σ integration in relation (23). Depending on the instrumental aberrations, this term may be complex and may therefore contribute a systematic phase term to the observed cross-spectrum phase. If we neglect instrumental aberrations and note that $\mathbf{q} - \Delta$ is approximately equal to $\mathbf{q}$, we obtain

$$\int\int W\left(\frac{\sigma+\mathbf{q}}{2}\right) W^*\left(\frac{\sigma-\mathbf{q}}{2}\right) W^*\left(\frac{\sigma+\mathbf{q}-\Delta}{2}\right) \times W\left(\frac{\sigma-\mathbf{q}+\Delta}{2}\right) \mathrm{d}\sigma \approx S_0(\mathbf{q}), \quad (24)$$

where $S_0(\mathbf{q})$ is the diffraction-limited transfer function of the instrument.

The integration over δ can be performed by using the substitutions

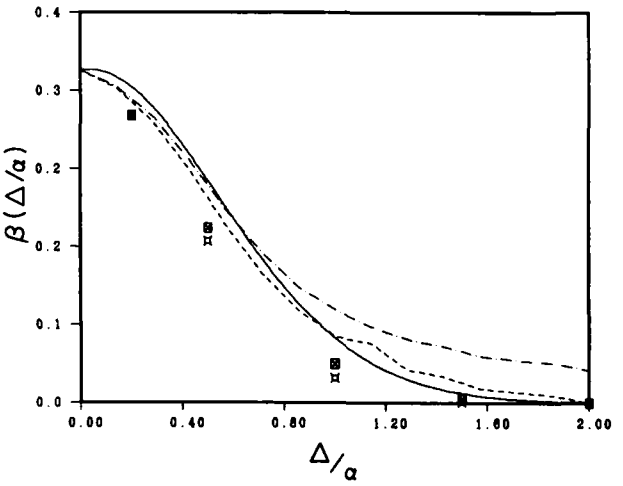

Fig. 2. Decay of signal in the cross-spectrum transfer as a function of $|\Delta|/\alpha$. Solid line, approximate result $\beta(\Delta/\alpha)$, [Eq. (26)]; □ and ⌗, ratios of the CTF models and the STF models for $\xi = 0$ and $\xi = 90$ deg, respectively, averaged over the spatial-frequency range from −0.8 to 0.8 and multiplied by 0.342; dotted–dashed line, measurement of C_τ,[17] multiplied by 0.342; dashed line, measurement of C_τ,[17] with a constant 0.1 subtracted and then multiplied by 0.342.

$$\rho = \frac{\delta}{\alpha}, \qquad \eta = \frac{\Delta}{2\alpha}, \qquad d\delta = \alpha^2 d\rho; \tag{25}$$

thus, inserting Eqs. (25) into the δ integral and using Eq. (6), we obtain

$$\int\int \exp\left\{-3.44\left[\left(\frac{|\delta + \Delta/2|}{\alpha}\right)^{5/3} + \left(\frac{|\delta - \Delta/2|}{\alpha}\right)^{5/3}\right]\right\} d\delta$$

$$= \alpha^2 \int\int \exp[-3.44(|\rho + \eta|^{5/3} + |\rho - \eta|^{5/3})] d\rho. \tag{26}$$

The value of the integral in Eq. (26) is a factor β that depends on Δ/α. The numerical calculation of $\beta(\Delta/\alpha)$ is presented in Fig. 2. Combining relation (24) and Eq. (26), we obtain, for the signal transfer function in the high-frequency approximation,

$$\mathrm{CTF}_\Delta(\mathbf{q})_{|\mathbf{q}| \gg \alpha} \approx \alpha^2 \beta\left(\frac{\Delta}{\alpha}\right) S_0(\mathbf{q}). \tag{27}$$

4. Combination of Approximate Results

A simple approximation to the overall signal transfer function is given by combining relations (20) and (27):

$$\mathrm{CTF}_\Delta(\mathbf{q}) = S_{\mathrm{LE}}(\mathbf{q}) S_{\mathrm{LE}}(\mathbf{q} - \Delta) + \alpha^2 \beta\left(\frac{\Delta}{\alpha}\right) S_0(\mathbf{q}). \tag{28}$$

The transfer function may be represented by the sum of two components, one describing the low-frequency portion and the other one describing the high-frequency regime. A similar approximation exists for the transfer function $\mathrm{STF}(\mathbf{q})$ of the Labeyrie signal,[11] which is reproduced if Δ is set to zero in Eq. (28):

$$\mathrm{STF}(\mathbf{q}) = S_{\mathrm{LE}}{}^2(\mathbf{q}) + 0.342\alpha^2 S_0(\mathbf{q}). \tag{29}$$

C. Numerical Calculations of Signal Transfer Functions

Equation (11) was evaluated numerically, assuming an aberration-free, unocculted circular entrance pupil [Eq. (14)]. The δ integration is carried out by a simple quadrature algorithm, in which the coordinate δ is represented by its magnitude d and the angle γ that δ makes with $\mathbf{q}$, so a polar coordinate system is used. The integration along d is performed first. A two-step procedure is applied to determine the integrand. First, the value of the exponential in Eq. (11) is calculated. The result is compared with the approximate value of the transfer function at large spatial frequencies: $\alpha^2\beta(\Delta/\alpha)$. If the result is smaller than a certain fraction of the approximate value (10^{-4} at the present time) it is considered insignificant, and the next step is omitted. This procedure speeds up the computation considerably while maintaining reasonable accuracy that is sensitive to the magnitude of Δ.

In the next step the σ integral is calculated. The integral is represented by the area that four circles of radius 1/2 and with centers located at $-(\mathbf{q} + \delta)/2$, $(\mathbf{q} - \delta)/2$, $(\delta - \mathbf{q} + \Delta)/2$, and $(\delta + \mathbf{q} - \Delta)/2$ have in common. The configuration is indicated in Fig. 1. Because of the presence of the frequency shift Δ, the situation is more complicated than in Korff's[9] case, and the symmetry of the problem is partially destroyed. The outer integration over γ must be carried out from 0 to π, instead of from 0 to $\pi/2$ as in Korff's case.

Because of the more complicated situation, an approach different from Korff's[9] was used in order to calculate the overlap area. Depending on the configuration of the circle

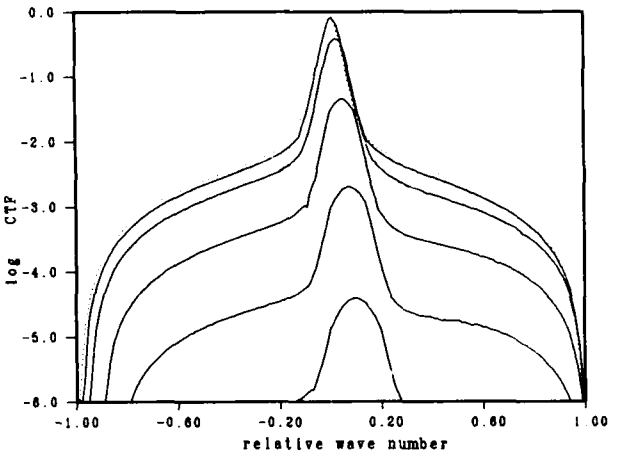

Fig. 3. CTF models by numerical evaluation of Eq. (11), for $\xi = 0$ deg and $\alpha = 0.1$. Dotted line, Labeyrie case (STF); solid lines, models for (in descending order of the curves) $|\Delta| = 0.02, 0.05, 0.1, 0.15, 0.2$. For negative relative wave numbers, the curves represent CTF models for $\xi = \pi$.

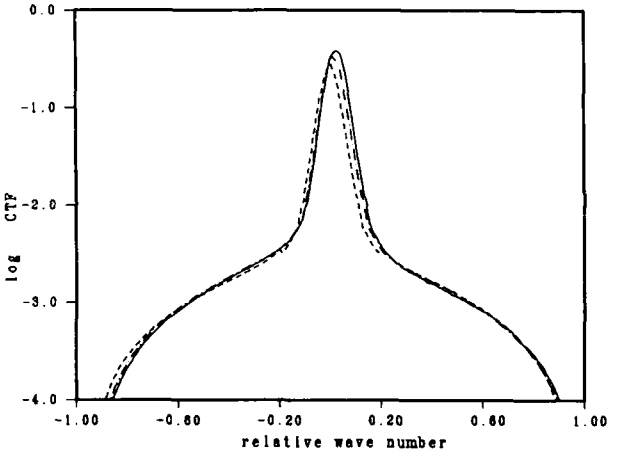

Fig. 4. CTF models by numerical evaluation of Eq. (11), for $|\Delta| = 0.05$ and $\alpha = 0.1$. Solid line, $\xi = 0$; dotted–dashed line, $\xi = \pi/4$; dashed line, $\xi = \pi/2$.

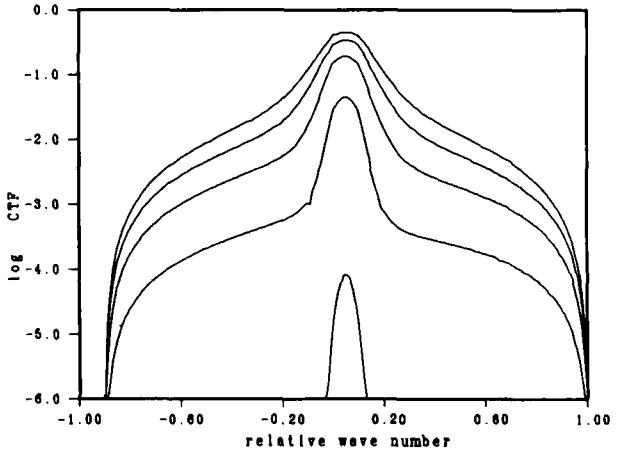

Fig. 5. CTF models by numerical evaluation of Eq. (11). In all cases, $\Delta = 1$ and $\xi = 0$. In descending order of the curves, $\alpha = 0.05, 0.1, 0.15, 0.2, 0.25$.

centers, the overlap area can be the area that two, three, or four circles have in common. First, the coordinates of the circle centers are calculated for a given set of values for d and γ. The two circles that have the largest separation of their centers are determined, and the locations of their points of intersection are calculated. Based on the distance of these intersection points to the centers of the other two circles, the program decides whether two, three, or four circles determine the overlap area and which ones are the relevant intersection points. Finally, the overlap is computed by combining the areas of triangles, quadrangles, and circular segments. For the case of circular segments, the area is taken from a lookup table rather than being computed in order to avoid calls to inverse trigonometric functions. The approach described here results in a relatively short and simple C source code that avoids frequent calculations of trigonometric function values.

Numeric results are presented in Figs. 3–5. Because of the frequency shift Δ, the transfer functions are no longer radially symmetric in $\mathbf{q}$ space, and they depend on the angle ξ that $\mathbf{q}$ makes with Δ. Figure 3 presents the results for $\xi = 0$; the curve parameter is the magnitude of Δ. Figure 4 presents the results for $\xi = 0$, for $\xi = \pi/4$, and for $\xi = \pi/2$, while Δ is 0.05. In all cases, α is 0.1, which corresponds to moderately good seeing for a meter-class telescope. Figure 5 presents results for a fixed magnitude of Δ and for varying seeing parameter α and demonstrates the loss of signal with increasing influence of turbulence.

4. DISCUSSION

Figures 3–5 indicate the properties of the signal transfer function for KT cross spectra. The loss of circular symmetry of the CTF is caused by the anisotropy of the problem, owing to the presence of the frequency shift Δ; the CTF has symmetry of reflection about the Δ direction. The maximum of the curves moves toward larger spatial frequencies in the direction of Δ. The signal decreases dramatically as $|\Delta|$ increases, under otherwise similar conditions. This behavior reflects the decorrelation of the phase contribution of the atmosphere to the instantaneous optical transfer function [Eq. (4)] over scales of order r_0/D.

Figure 2 shows the loss of signal as a function of $|\Delta|$ in various ways. The solid curve represents the factor β, which appears in the approximation of the CTF for large spatial frequencies. The solid markers represent suitable averages of ratios of model CTF's for various values for Δ and the signal transfer function calculated for $\xi = 0$ and $\xi = 90$ deg and multiplied by a constant 0.342. The dashed lines show measurements of the decrease of the KT signal that were made by Karo and Schneidermann.[17] The data were taken from the curve labeled C_7 in Fig. 3 of Ref. 17. One of the dashed curves represents the data from Ref. 17 but with a constant tentatively subtracted in order to account for possible measurement noise. In any case, the numeric models, the approximation, and the measurements agree to a good extent. It is seen from Fig. 2 that for finite Δ the signal in the KT cross spectra is always smaller than the signal for the Labeyrie case $\Delta = 0$. However, the requirements for the magnitude of Δ appear to be less stringent than was previously believed. In the approximation, the signal has half the magnitude of the Labeyrie signal if $\Delta = 0.6\,\alpha$, and even for $\Delta = \alpha$ the signal in the cross spectra has some 20% of the Labeyrie signal.

These results may be used to estimate the influence of instrumental noise on the phases of the cross spectra. To do this, we shall extend the treatment of the problem described by Deron and Fontanella.[18] They assumed a zero-mean, complex Gaussian additive-noise contribution with a variance σ_N^2 to the Fourier transforms of the individual frames. They showed that the variance $\sigma_{\phi_i}^2$ of the cross-spectrum phase ϕ_i of a single frame i can be expressed as

$$\sigma_{\phi_i}^2 = \frac{\sigma_{\mathrm{Im}[F_i(\mathbf{q})F_i^*(\mathbf{q}-\Delta)]}^2}{[|F_0(\mathbf{q})|^2\mathrm{STF}(\mathbf{q})]^2}, \tag{30}$$

if the noise-free cross-spectrum phase is arbitrarily set to zero. Im(·) denotes the imaginary part of a complex number. It is assumed in Eq. (30) that the noise amplitude is small compared with the signal amplitude and that, because $|\Delta|$ is small, the observed signal magnitude in the denominator is well represented by the signal of the Labeyrie case $\Delta = 0$. I shall drop the latter assumption and replace the denominator by the proper term,

$$\sigma_{\phi_i}^2 = \frac{\sigma_{\mathrm{Im}[F_i(\mathbf{q})F_i^*(\mathbf{q}-\Delta)]}^2}{[|F_0(\mathbf{q})F_0^*(\mathbf{q}-\Delta)|\mathrm{CTF}_\Delta(\mathbf{q})]^2}. \tag{31}$$

In addition, Deron and Fontanella showed that the variance of the imaginary part of the observed cross spectrum $F_i(\mathbf{q})F_i^*(\mathbf{q}-\Delta)$ is approximately

$$\sigma_{\mathrm{Im}[F_i(\mathbf{q})F_i^*(\mathbf{q}-\Delta)]}^2 \approx \sigma_N^2|F_0(\mathbf{q})|^2\mathrm{STF}(\mathbf{q}), \tag{32}$$

and hence

$$\sigma_{\phi_i}^2 \approx \frac{\sigma_N^2|F_0(\mathbf{q})|^2\mathrm{STF}(\mathbf{q})}{[|F_0(\mathbf{q})F_0^*(\mathbf{q}-\Delta)|\mathrm{CTF}_\Delta(\mathbf{q})]^2} \tag{33}$$

for a single frame or

$$\sigma_{\phi_i}^2 \approx \frac{1}{N}\frac{\sigma_N^2|F_0(\mathbf{q})|^2\mathrm{STF}(\mathbf{q})}{[|F_0(\mathbf{q})F_0^*(\mathbf{q}-\Delta)|\mathrm{CTF}_\Delta(\mathbf{q})]^2} \tag{34}$$

for an average of N cross spectra.

If we assume that the modulus of the object spectrum $F_0(\mathbf{q})$ does not vary rapidly over frequency scales of order Δ (which is essentially true when the observed object has only a small spatial extent), we may set $|F_0(\mathbf{q})F_0^*(\mathbf{q}-\Delta)| \approx |F_0(\mathbf{q})|^2$, and we obtain

$$\sigma_{\phi_i}^2 \approx \frac{1}{N}\frac{\sigma_N^2}{|F_0(\mathbf{q})|^2}\frac{\mathrm{STF}(\mathbf{q})}{[\mathrm{CTF}_\Delta(\mathbf{q})]^2}. \tag{35}$$

A good representation of the signal-to-noise ratio SNR of the Labeyrie signal is given by[19]

$$\mathrm{SNR}(\mathbf{q}) = \frac{|F_0(\mathbf{q})|^2\mathrm{STF}(\mathbf{q})}{\sigma_N^2}, \tag{36}$$

so we finally obtain

$$\sigma_{\phi_i}^2 \approx \frac{1}{N}\frac{1}{\mathrm{SNR}(\mathbf{q})}\left[\frac{\mathrm{STF}(\mathbf{q})}{\mathrm{CTF}_\Delta(\mathbf{q})}\right]^2. \tag{37}$$

If the signal-to-noise ratio of the Labeyrie signal is known, relation (37) may be used to estimate the contribution of noise to the error of cross-spectrum phases and therefore to the error in the reconstructed phase. To illustrate this, let us assume a simple, practical case in which image Fourier transforms are known along only one spatial-frequency dimension. Data of this type are obtained if, e.g., the speckle pattern of a resolved source in the focal plane of an infrared telescope is scanned by using a narrow slit followed by a single infrared detector.[20] For a given frequency spacing Δ, the cross spectrum phase ϕ_k is given at discrete spatial frequencies $\mathbf{q}_k = (0, \Delta, 2\Delta, \ldots, k\Delta, \ldots, K\Delta)$, where K is the largest integer number smaller than $1/\Delta$. Object phases ψ_k can be recovered at the same discrete frequencies by applying a simple summation algorithm:

$$\psi_k = \psi_{k-1} + \phi_k, \qquad \psi_0 = 0 \qquad \text{or} \qquad \psi_k = \sum_{j=1}^{k} \phi_j. \tag{38}$$

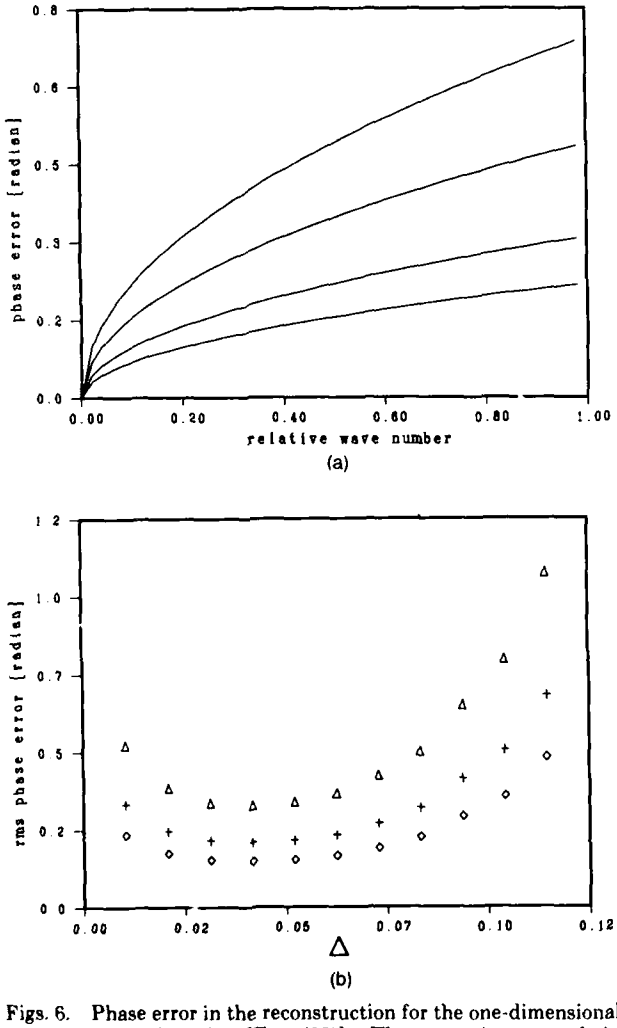

Figs. 6. Phase error in the reconstruction for the one-dimensional reconstruction algorithm [Eqs. (38)]. The approximate result in Eq. (26) was used for the STF/CTF ratio in Eq. (37). (a) Phase error as a function of frequency for $|\Delta| = 0.02$ and $\alpha = 0.1$ and values for the product of SNR and the frame number N of (in descending order of the curves) 100, 200, 500, and 1000. (b) Reconstructed rms phase error averaged over all spatial frequencies as a function of $|\Delta|$, for $\alpha = 0.1$. N(SNR) values: Δ, 200; +, 500; ◇, 1000.

The variance of the error of the reconstructed object phase is given by the sum of the error variances of the cross-spectrum phase values that were added to arrive at a given object phase, and it therefore increases with increasing frequency index. Figure 6(a) represents the resulting rms error of the reconstructed object phase, assuming a frequency-independent signal-to-noise ratio.

The proper choice of the magnitude of Δ results in optimally small rms phase errors, as illustrated in Fig. 6(b). The rms object phase error is presented as a function of Δ, and it is seen that for otherwise fixed conditions, the rms error has a minimum for a certain value of the frequency shift. For small Δ, the cross-spectrum error is small, but many summations are required in order to arrive at a given frequency, while for large Δ, the cross-spectrum errors by themselves are large. Although the optimal choice for Δ is 0.4α, the rms phase error remains fairly small over a wide range. Therefore I conclude that the magnitude of Δ may be chosen within the range from $\Delta = 0.2\alpha$ to $\Delta = 0.8\alpha$ without introducing severe phase errors due to random noise into the reconstruction.

Another application of the results presented here is the recovery of the full object Fourier transform from the KT cross spectra. Although the KT algorithm is applied mainly to recover object phases, object amplitudes can be obtained as well if cross spectra are calibrated properly for seeing effects. The main advantage is that average power spectra no longer need to be calculated, which may be a matter of concern if the algorithm is to be applied in real time. If a quick-look reconstruction is all that is asked for or if a suitable reference source is missing but r_0 is known, the amplitude recalibration can be done by using the models presented here. The reconstruction algorithm that applies to the simple, one-dimensional case discussed above is given by

$$F_{o,k} = \frac{\langle F_{i,k} F^*_{i,k-1} \rangle}{\mathrm{CTF}_{\Delta,k} F^*_{o,k-1}}, \qquad F_{o,0} = 1, \tag{39}$$

where $\langle F_{i,k} F^*_{i,k-1} \rangle$ represents the observed cross spectrum at a frequency index k, $\mathrm{CTF}_{\Delta,k}$ is the CTF value at that index, and $F_{o,k}$ represents the reconstructed Fourier-transform value.

APPENDIX A: EXTENSION OF KORFF'S ANALYSIS TO THE KNOX-THOMPSON TECHNIQUE

We begin the analysis with Eq. (10) of Subsection 3.A:

$$\begin{aligned}\mathrm{CTF}_\Delta(\mathbf{q}) = \Big\langle \int\int & W(\mathbf{r} + \mathbf{q}/2) W^*(\mathbf{r} - \mathbf{q}/2) \\ & \times \exp\{j[\phi(\mathbf{r} + \mathbf{q}/2) - \phi(\mathbf{r} - \mathbf{q}/2)]\} d\mathbf{r} \\ & \times \int\int W^*[\mathbf{r}' + (\mathbf{q} - \Delta)/2] W[\mathbf{r}' - (\mathbf{q} - \Delta)/2] \\ & \times \exp(j[-\phi[\mathbf{r}' + (\mathbf{q} - \Delta)/2] \\ & + \phi[\mathbf{r}' + (\mathbf{q} - \Delta)/2]]) d\mathbf{r}' \Big\rangle .\end{aligned}$$

We rewrite the product of integrals as multiple integrals,

regroup factors, and perute integration and ensemble averaging:

$$\mathrm{CTF}_\Delta(\mathbf{q}) = \int\int\int\int W(\mathbf{r}+\mathbf{q}/2)W^*(\mathbf{r}-\mathbf{q}/2) \times W^*[\mathbf{r}'+(\mathbf{q}-\Delta)/2]W[\mathbf{r}'-(\mathbf{q}-\Delta)/2] \times \langle \exp(j\{\phi(\mathbf{r}+\mathbf{q}/2)-\phi(\mathbf{r}-\mathbf{q}/2) - \phi[\mathbf{r}'+(\mathbf{q}-\Delta)/2]+\phi[\mathbf{r}'-(\mathbf{q}-\Delta)/2]\})\rangle \mathrm{d}\mathbf{r}\mathrm{d}\mathbf{r}'. \quad (A1)$$

The next step involves the evaluation of the ensemble average in Eq. (A1). Similar expressions were treated by Fried[10] and by Korff.[9] A brief justification of those treatments is given by Roddier (Ref. 11, p. 293). We state the result:

$$\langle \exp(j\{\phi(\mathbf{r}+\mathbf{q}/2)-\phi(\mathbf{r}-\mathbf{q}/2)-\phi[\mathbf{r}'+(\mathbf{q}-\Delta)/2]+\phi[\mathbf{r}'-(\mathbf{q}-\Delta)/2]\})\rangle = \exp(-\tfrac{1}{2}\langle\{\phi(\mathbf{r}+\mathbf{q}/2)-\phi(\mathbf{r}-\mathbf{q}/2)-\phi[\mathbf{r}'+(\mathbf{q}-\Delta)/2]+\phi[\mathbf{r}'-(\mathbf{q}-\Delta)/2]\}^2\rangle). \quad (A2)$$

We next analyze Eq. (A2) in order to express the phases ϕ in terms of structure functions. Partial evaluation of the square in the right-hand side of Eq. (A2) results in

$$\begin{aligned}\langle\{\phi(\mathbf{r}+\mathbf{q}/2)-\phi(\mathbf{r}-\mathbf{q}/2)-\phi[\mathbf{r}'+(\mathbf{q}-\Delta)/2]+\phi[\mathbf{r}'-(\mathbf{q}-\Delta)/2]\}^2\rangle &= \langle[\phi(\mathbf{r}+\mathbf{q}/2)-\phi(\mathbf{r}-\mathbf{q}/2)]^2\rangle + \langle\{\phi[\mathbf{r}'+(\mathbf{q}+\Delta)/2] - \phi[\mathbf{r}'-(\mathbf{q}-\Delta)/2]\}^2\rangle - \langle 2\phi(\mathbf{r}+\mathbf{q}/2)\phi[\mathbf{r}'+(\mathbf{q}-\Delta)/2]\rangle \\ &- \langle 2\phi(\mathbf{r}-\mathbf{q}/2)\phi[\mathbf{r}'+(\mathbf{q}-\Delta)/2]\rangle \\ &+ \langle 2\phi(\mathbf{r}-\mathbf{q}/2)\phi(\mathbf{r}'+(\mathbf{q}-\Delta)/2)\rangle \\ &+ \langle 2\phi(\mathbf{r}+\mathbf{q}/2)\phi[\mathbf{r}'+(\mathbf{q}-\Delta)/2]\rangle. \end{aligned} \quad (A3)$$

The first two terms in Eq. (A3) are already structure function terms. The other four terms may be rewritten in structure functions if Eq. (A3) is expanded by the following terms, which add to zero:

$$\begin{aligned}&\langle\phi^2(\mathbf{r}+\mathbf{q}/2)\rangle + \langle\phi^2(\mathbf{r}'+(\mathbf{q}-\Delta)/2)\rangle + \langle\phi^2(\mathbf{r}-\mathbf{q}/2)\rangle \\ &+ \langle\phi^2(\mathbf{r}'-(\mathbf{q}+\Delta)/2)\rangle - \langle\phi^2(\mathbf{r}+\mathbf{q}/2)\rangle \\ &- \langle\phi^2(\mathbf{r}'+(\mathbf{q}-\Delta)/2)\rangle - \langle\phi^2(\mathbf{r}-\mathbf{q}/2)\rangle \\ &- \langle\phi^2[\mathbf{r}'-(\mathbf{q}+\Delta)/2]\rangle. \end{aligned} \quad (A4)$$

Now, by using Eq. (5), Eq. (A3) becomes

$$\begin{aligned}\langle\{\phi(\mathbf{r}+\mathbf{q}/2)-\phi(\mathbf{r}-\mathbf{q}/2)-\phi[\mathbf{r}'+(\mathbf{q}-\Delta)/2]+\phi[\mathbf{r}'-(\mathbf{q}-\Delta)/2]\}^2\rangle &= \langle[\phi(\mathbf{r}+\mathbf{q}/2)-\phi(\mathbf{r}-\mathbf{q}/2)]^2\rangle + \langle\{\phi[\mathbf{r}'+(\mathbf{q}+\Delta)/2]-\phi[\mathbf{r}'-(\mathbf{q}-\Delta)/2]\}^2\rangle \\ &+ \langle[\phi(\mathbf{r}+\mathbf{q}/2)-\phi[\mathbf{r}'+(\mathbf{q}-\Delta)/2]]^2\rangle \\ &+ \langle\{\phi(\mathbf{r}-(\mathbf{q}/2)-\phi[\mathbf{r}'+(\mathbf{q}-\Delta)/2]\}^2\rangle \\ &- \langle[\phi(\mathbf{r}-\mathbf{q}/2)-\phi(\mathbf{r}'+(\mathbf{q}-\Delta)/2)]^2\rangle \\ &- \langle[\phi(\mathbf{r}+(\mathbf{q}/2)-\phi(\mathbf{r}'-(\mathbf{q}-\Delta)/2)]^2\rangle \\ &= \mathbf{D}(\mathbf{q})+\mathbf{D}(\mathbf{q}-\Delta)+\mathbf{D}(\mathbf{r}-\mathbf{r}'+\Delta/2) \\ &+ \mathbf{D}(\mathbf{r}-\mathbf{r}'-\Delta/2)-\mathbf{D}(\mathbf{q}+\mathbf{r}-\mathbf{r}'-\Delta/2) \\ &- \mathbf{D}(\mathbf{q}-\mathbf{r}+\mathbf{r}'-\Delta/2). \end{aligned} \quad (A5)$$

Inserting Eqs. (A5) and (A2) into Eq. (A1) yields

$$\mathrm{CTF}_\Delta(\mathbf{q}) = \int\int\int\int W(\mathbf{r}+\mathbf{q}/2)W^*(\mathbf{r}-\mathbf{q}/2) \times W^*(\mathbf{r}'+(\mathbf{q}-\Delta)/2)W[\mathbf{r}'-(\mathbf{q}-\Delta)/2] \times \exp\{-\tfrac{1}{2}[\mathbf{D}(\mathbf{q})+\mathbf{D}(\mathbf{q}-\Delta)+\mathbf{D}(\mathbf{r}-\mathbf{r}'+\Delta/2) + \mathbf{D}(\mathbf{r}-\mathbf{r}'-\Delta/2)-\mathbf{D}(\mathbf{q}+\mathbf{r}-\mathbf{r}'-\Delta/2) - \mathbf{D}(\mathbf{q}-\mathbf{r}+\mathbf{r}'-\Delta/2)]\}\mathrm{d}\mathbf{r}\mathrm{d}\mathbf{r}'. \quad (A6)$$

The exponent in Eq. (A6) depends on only the difference $\mathbf{r}-\mathbf{r}'$. A change of variables is therefore made:

$$\sigma = \mathbf{r}+\mathbf{r}', \qquad \delta = \mathbf{r}-\mathbf{r}', \qquad \mathbf{r} = \frac{\sigma+\delta}{2}, \qquad \mathbf{r}' = \frac{\sigma-\delta}{2}. \quad (A7)$$

We then obtain the final, general result for the transfer function of KT cross spectra:

$$\mathrm{CTF}_\Delta(\mathbf{q}) = \int\int\int\int W\left(\frac{\sigma+\delta+\mathbf{q}}{2}\right)W^*\left(\frac{\sigma+\delta-\mathbf{q}}{2}\right) \times W^*\left(\frac{\sigma-\delta+\mathbf{q}-\Delta}{2}\right)W\left(\frac{\sigma-\delta-\mathbf{q}+\Delta}{2}\right)\mathrm{d}\sigma \times \exp\{-\tfrac{1}{2}[\mathbf{D}(\mathbf{q})+\mathbf{D}(\mathbf{q}-\Delta)+\mathbf{D}(\delta+\Delta/2) + \mathbf{D}(\delta-\Delta/2)-\mathbf{D}(\mathbf{q}-\Delta/2+\delta) - \mathbf{D}(\mathbf{q}-\Delta/2-\delta)]\}\mathrm{d}\delta.$$

ACKNOWLEDGMENTS

This research was done while the author held a National Research Council–U.S. Air Force Geophysics Laboratory Research Associateship. The suggestion by Christian Perrier (Observatoire de Lyon) to perform the noise analysis presented here is greatly appreciated. The numerical work was carried out on the VAX 750 computer at the National Solar Observatory in Sunspot, New Mexico.

REFERENCES

1. K. T. Knox and B. J. Thompson, "Recovery of images from atmospherically degraded short exposure photographs," Astrophys. J. **193**, L45–L48 (1974).
2. A. Labeyrie, "Attainment of diffraction-limited resolution in large telescopes by Fourier-analyzing speckle patterns in star images," Astron. Astrophys. **6**, 85–87 (1970).
3. G. Weigelt and B. Wirnitzer, "Image reconstruction by the speckle-masking method," Opt. Lett. **8**, 389–391 (1983).
4. P. Nisenson, R. V. Stachnik, M. Karovska, and R. W. Noyes, "A new optical source associated with T Tauri," Astrophys. J. **297**, L17–L20 (1985).
5. R. V. Stachnik, P. Nisenson, and R. W. Noyes, "Speckle image reconstruction of solar features," Astrophys. J. **271**, L37–L40 (1983).
6. D. L. Fried, "Angular dependence of the atmospheric turbulence effect in speckle interferometry," Opt. Acta **26**, 597–613 (1979).
7. O. von der Lühe, "High resolution speckle imaging of solar small scale structure: the influence of anisoplanatism," in *High Resolution in Solar Physics*, Vol. 233 of Lecture Notes in Physics, R. Muller, ed. (Springer-Verlag, Berlin, 1985), pp. 96–102.
8. C. Leinert and M. Haas, "Infrared speckle interferometry on Calar Alto," in *High Resolution Interferometric Imaging from the Ground*, Proceedings of the Joint European Southern Observatory–National Optical Astronomy Observatories Confer-

ence (National Optical Astronomy Observatories, Tucson, Ariz., 1987), pp. 233–236.
9. D. Korff, "Analysis of a method for obtaining near-diffraction-limited information in the presence of atmospheric turbulence," J. Opt. Soc. Am. **63,** 971–980 (1973).
10. D. L. Fried, "Optical resolution through a randomly inhomogeneous medium for very short and very long exposures," J. Opt. Soc. Am. **56,** 1372–1379 (1966).
11. F. Roddier, "The effects of atmospheric turbulence in optical astronomy," in *Progress in Optics*, E. Wolf, ed. (Elsevier, New York, 1981), Vol. XIX.
12. V. I. Tatarskii, *The Effects of the Turbulent Atmosphere on Wave Propagation*, (Israel Program for Scientific Translations, Jerusalem, 1971).
13. R. Barakat and P. Nisenson, "Influence of the wave-front correlation function and deterministic wave-front aberrations on the speckle image reconstruction problem," J. Opt. Soc. Am. **71,** 1390–1402 (1981).
14. J. B. Breckinridge, "Measurement of the amplitude of phase excursions in the earth's atmosphere," J. Opt. Soc. Am. **66,** 143–144 (1976).
15. C. Roddier, "Measurements of the atmospheric attenuation of the spectral components of astonomical images," J. Opt. Soc. Am. **66,** 478–482 (1976).
16. M. Bertolotti, M. Carnevale, A. Consortini, and L. Ronchi, "Optical propagation: problems and trends," Opt. Acta **26,** 507–529 (1979).
17. D. P. Karo and A. M. Schneidermann, "Transfer functions, correlation scales, and phase retrieval in speckle interferometry," J. Opt. Soc. Am. **67,** 1583–1587 (1977).
18. R. Deron and J. C. Fontanella, "Restauration d'images dégradées par la turbulence atmosphérique selon la méthode de Knox et Thompson," J. Opt. (Paris) **15,** 15–23 (1984).
19. O. von der Lühe and R. B. Dunn, "Solar granulation power spectra from speckle interferometry," Astron. Astrophys. **177,** 265–276 (1987).
20. J. D. Freeman, J. C. Christou, F. Roddier, D. W. McCarthy, Jr., and M. C. Cobb, "Application of triple correlation to one-dimensional infrared speckle data," in *High Resolution Interferometric Imaging from the Ground*, Proceedings of the Joint European Southern Observatory–National Optical Astronomy Observatories Conference (National Optical Astronomy Observatories, Tucson, Ariz., 1987), pp. 47–56.